Interdiscip Toxicol. 2020; **Vol. 13**(1): 1–12.
doi: 10.2478/intox-2020-0001

sciendo

interdisciplinary toxicology

REVIEW ARTICLE

Ozone decomposition – state of the art and new approaches

Todor BATAKLIEV [1], Vladimir GEORGIEV [1], Slavcho RAKOVSKY [1], Gennadi E. ZAIKOV [2]

[1] Institute of Catalysis, Bulgarian Academy of Sciences, Sofia, Bulgaria
[2] N.M. Emanuel Institute of Biochemical Physics, Russian Academy of Sciences, Moscow, Russia

ITX130120A01 • Received: 06 October 2019 • Accepted: 26 February 2020

ABSTRACT

The effective ozone decomposition is still a scientific challenge because of its rising industrial use in global scale. Wide application of high ozone concentrations forces researchers to work on new catalytic systems for ozone removal concerning mostly the surrounding human environment (airplane cabins, copiers, laser printers, sterilizers, *etc.*). It is not an easy task considering the fact that above concentration of 0.1 mg/m^3 the ozone could seriously harm human health. Current studies estimate a huge number of untimely deceased people per year on a global scale as a direct consequence of air pollution. It is imposing to reinforce the efforts in workable ozone decomposition on ground atmospheric layer as an important part of air purification process. This review comprises general look on basic physico-chemical properties of ozone completed by recently reported literature about catalytic ozone destruction. Discussion over kinetics and mechanisms of ozone decomposition reaction will be represented in order to do an attempt to clarify these most outstanding parts of the topic.

KEY WORDS: catalysts; synthesis; kinetics; mechanism; ozone; decomposition

Introduction

In last years, the scientific researchers from all over the world are trying to solve deep environmental problems on earth such as the global warming, water and air pollution. A main factor affecting negatively these processes is the presence of ozone on ground level in many overpopulated cities that is a result of its large industrial synthesis and application (Batakliev *et al.*, 2014). The outdoor ozone break-in into buildings is a threat causing health effects such as decreased lung function and respiratory symptoms (Lai *et al.*, 2015). A number of large-scale studies have found a serious relationship between human mortality and outdoor/indoor ozone exposure (Chen *et al.*, 2012). Contrariwise, the atmospheric ozone, so precious for every living being, is situated mostly in the so-called "ozone layer" from 15 to 30 km above the earth surface wherein the ozone concentration is in the range 10–20 (Ulmann, 1991). The ozone synthesis in the stratosphere runs photochemically by means of solar radiation impact on molecular oxygen (Rakovsky *et al.*, 2007). The atmospheric ozone is really valuable to everything alive on Earth thanks to ozone property to absorb the hard UV-B and UV-C sun radiation in the wavelength range 220–310 nm. The study of kinetics and mechanism of ozone reactions in modern science is closely related to solving the ozone gap problem despite the positive trend of ozone layer recovery in recent years (Figure 1).

The catalytic ozone decomposition on the surface of diverse oxides based on transition metals as well as the use of catalysts modified with noble metals is much more green and low cost method then other techniques as thermal ozone destruction or gas rarefaction by massive air compressors.

Physico-chemical properties and synthesis of ozone

The ozone molecule consists of three oxygen atoms with length of each O-O-bond: $\rho_{o\text{-}o}$ = 1.278 Å and blunt angle between the oxygen bonds of 116.8°. Ozone can get through into each physical state but at normal conditions, the ozone is colorless gas with sharp odor. When the ozone concentration is more than 15–20% it has blue color. At atmospheric pressure and temperature of

Correspondence address:
Dr. Todor Batakliev
Institute of Catalysis,
Bulgarian Academy of Sciences, Sofia, Bulgaria
E-MAIL: todorbat@gmail.com

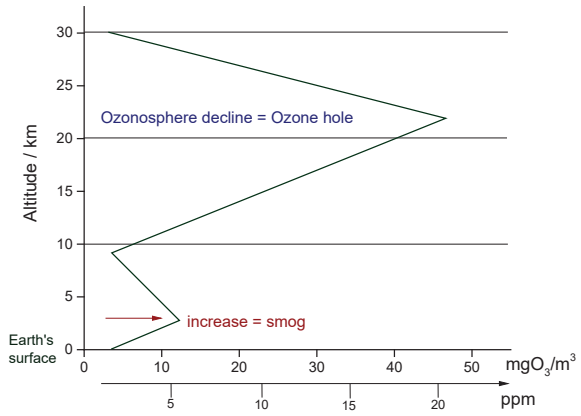

Figure 1. Atmospheric ozone concentration depending on altitude.

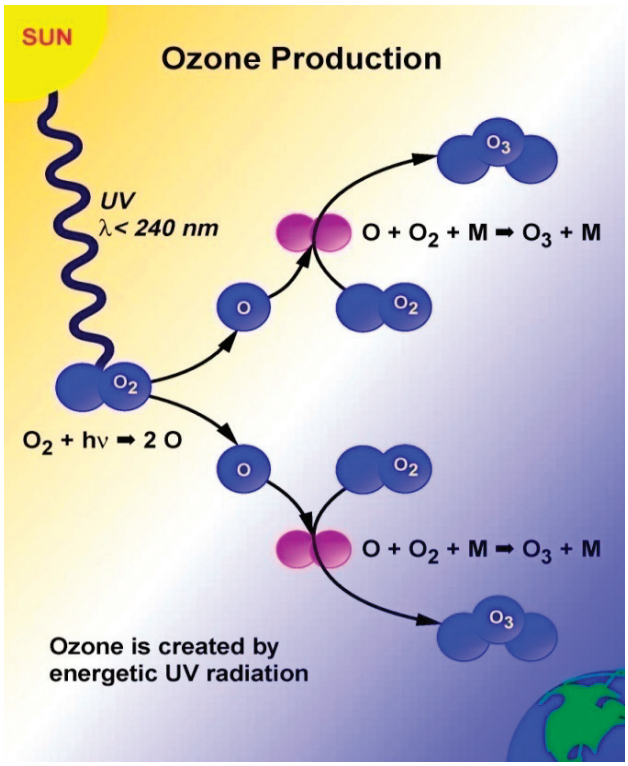

Figure 2. Stratospheric ozone synthesis.

161.3 K, the ozone becomes liquid in deep blue color. It turns into solid at 80.6 K by acquiring dark purple color (Lunin *et al.,* 1998). The risk of ozone detonation is a function of its thermodynamic instability ($\Delta G°298 = -163$ kJ/mol), moreover its decomposition to diatomic oxygen is a thermodynamically conducive process with heat of reaction $\Delta H°298 = -138$ kJ/mol (Perry & Green, 1989).

The creation of ozone in the atmosphere is running photochemically at altitude between 20 and 30 km under the influence of solar UV radiation (wavelength <240 nm). Thereby the ozone concentration is uniformly in the range 10–20 ppm (Figure 2).

For industrial purposes, ozone is synthesized by using pure oxygen by thermal, photochemical, chemical, electrochemical methods, in all forms of electrical discharge

Table 1. Equilibrium constant (K_e) of reaction (2) depending on the temperature

T, K	1500	2000	3000	4000	5000	6000
K_e, M	$1{,}662.10^{-11}$	$4{,}413.10^{-7}$	$1{,}264.10^{-2}$	2.104	48.37	382.9

and under action of a particles stream (Batakliev *et al.,* 2014). The synthesis of ozone is carried out by the following reactions shown in the scheme:

$$O_2 + (e^-, h\nu, T) \rightarrow 2O\ (O_2^*) \quad (1)$$

$$O_2 + O + M \leftrightarrow O_3 + M \quad (2)$$

$$O_2^* + O_2 \rightarrow O_3 + O \quad (3)$$

Where: M is each third particle.

At low temperatures, the ozone consists mainly of molecular oxygen and at higher temperatures of atomic oxygen. There is no area of temperatures at normal pressure wherein the ozone partial pressure is significant. The maximum steady-state pressure, observed at temperature of 350 K, is only 9.10^{-7} bar. The values of the equilibrium constant of reaction (2) at different temperatures are presented in Table 1 (Hon & Yan, 1993).

At high temperatures, when the concentration of atomic oxygen is high, the equilibrium of reaction (2) is moved to the left and the ozone concentration is low. At low temperatures, the equilibrium is shifted to the right but because of the low atomic oxygen concentration the ozone content is negligible. For synthesis of significant ozone concentrations it is always necessary to have the following conditions: 1) low temperature and 2) formation of superequilibrium concentrations of atomic oxygen. Ozone could be formed at low temperatures every time when a process of oxygen dissociation is running. Photochemical synthesis of ozone occurs upon irradiation of gaseous or liquid oxygen by UV radiation with wavelength λ<210 nm (Deninno & McCarthy, 1997). It was suggested (Claudia *et al.,* 1994), that the formation of ozone in presence of radiation with wavelength in the range of $175<\lambda<210$ may be associated with the formation of excited oxygen molecules:

$$O_2 + h\nu \rightarrow (O_2^*) \quad (4)$$

$$O_2^* + O_2 \rightarrow O_3 + O \quad (5)$$

$$O_2 + O + M \leftrightarrow O_3 + M \quad (6)$$

The photochemical ozone synthesis has an important role in atmospheric processes, but it is not easy to apply it for industrial application because of the high energy costs (32 kWh/kg ozone) for generating high-energy shortwave radiation. Nowadays the industrial synthesis of ozone happens mostly by means of electric discharge methods consisting of passing oxygen containing gas through high-voltage (8–10 kV) electrodes. That way, as result of collisions between oxygen molecules and accelerated electrons, part of the kinetic energy is transformed in dissociation energy of O-O bond and formation of excited oxygen molecules at the same time (Rakovsky *et al.,* 2007; Lunin *et al.,* 1998). It is an important precondition before the final step when two molecules of oxygen create one oxygen atom and one ozone molecule:

$O_2 + e \rightarrow 2O\ (O_2^*)$ (7)
$O_2 + O + M \rightarrow O_3 + M$ (8)
$O_2^* + O_2 \leftrightarrow O_3 + O$ (9)

Catalytic ozone decomposition in gas phase

The process of ozone decomposition on the surface of solids is of great interest because of its industrial application. Along with the known gas cycles depleting the atmospheric ozone, the ozone decomposition plays a significant role over aerosols, which their quantity is always a risk due to the anthropogenic factor. The growth of ozone used in chemical industries set up the task for destruction of the residual ozone on heterogeneous environmentally friendly catalysts. In humid environments, under certain temperatures and gas flow rates, this catalytic process, as well as the reaction mechanism, has not been yet fully studied and clarified. The ozone has a great number of advantages as oxidizing agent and, in that ability, it has been used in different scientific investigations done with neutralization of volatile organic contaminants (Skoumal *et al*., 2006; Bianchi *et al*., 2006) as in presence of catalyst the ozonation efficiency is rising (Ma *et al*., 2004; Zhao *et al*., 2008).

The noble metal catalysts and the oxide catalysts based on transition metals have been widely used as catalytic systems for ozone decomposition (Hata *et al*., 1988; Tchihara, 1988; Kobayashi *et al*., 1988; Terui *et al*., 1990; Terui *et al*., 1991; Oohachi *et al*., 1993). The main metals used by the authors were Pt, Pd, Rh and Ce, as well as, metals or metal oxides of Mn, Co, Fe, Ni, Zn, Ag and Cu. The significant price of the noble metals increases the application of metal oxide catalysts having carriers with high specific surface such as γ-Al_2O_3, SiO_2, TiO_2, ZrO_2 and charcoal. Many researchers focused on the development, study and application of catalysts for ozone decomposition based on supported or mixed metal oxides because of the expensive cost of metals as platinum, gold and palladium. In this connection have been the most considerably investigated the oxides of Mn, Co, Cu, Fe, Ni, Si, Ti, Zr, Ag and Al (Oyama, 2000; Einaga & Futamura, 2004; Radhakrishnan *et al*., 2001; Zavadskii *et al*., 2002). It was found that oxide compounds based on transition metals exhibit highest catalytic activity in ozone decomposition (Batakliev *et al*., 2017), and especially the catalysts based on manganese oxide (Batakliev *et al*., 2008). The effect of nickel content in the catalyst was investigated in our paper (Batakliev *et al*., 2017) in terms to elucidate the catalytic activity, stability and mechanical strength of the mixed metal oxides generated by thermal treatment of co-precipitated Ni-Cu-Al samples as catalyst precursors in the reaction of ozone decomposition. The impact of the silver present as a promoter on the catalytic activity was also examined. It could be suggested that during ozone decomposition on transition metal oxides such as NiO-CuO-Al_2O_3 there is formation of intermediate ionic particles possessing either superoxide or peroxide features. The formation of charged chemisorbed oxygen species is accompanied by oxidation of an appropriate number of cations in the oxide crystal lattice to a higher state. In this case it will be the oxidation of Ni^{2+} to Ni^{3+} ions, *scilicet*:

$O_3 + Ni^{2+} \rightarrow O^{2-} + Ni^{3+} + O_2$ (10)
$O_3 + O^{2-} + Ni^{3+} \rightarrow O_2^{2-} + Ni^{3+} + O_2$ (11)
$O_2^{2-} + Ni^{3+} \rightarrow Ni^{2+} + O_2$ (12)

The probable reaction scheme of ozone decomposition consists of electron transfer from the Ni^{2+} center to ozone, resulting in formation of higher oxidation Ni^{3+} species and peroxide particles O_2^{2-}, followed by reduction of Ni^{3+} species by desorption of peroxide particle to form oxygen ($O_2^{2-} \rightarrow O_2 + 2e^-$).

The dissociation of ozone molecules over the surface of metal oxide catalyst based on manganese, nickel and copper oxides was performed by means of kinetic study concerning the equation solution for γ coefficient and activation energy outcome of the process (Batakliev *et al*., 2008). The excellent activity of this catalyst was confirmed by the high values of the coefficient γ found out to be in the range $(2.5–3.5)\times10^{-4}$. Even in humid environment, the decline of catalytic activity did not exceed 20% measured by coefficient values. Following the changes of γ at two different flow rates in the temperature range of 258–323K and using the Arrhenius equation, the calculated activation energy of ozone decomposition reaction was 5 kJ.mol^{-1}. It means that between ozone molecules and catalytic surface appear weak Van der Waals forces and there is running of physisorption during the reaction. Desorption of intermediate species and oxygen molecules is going relatively lightly in expense of the energy shed by catalyst crystal lattice. In another article concerning redox catalytic process in the presence of heterogeneous catalyst (Batakliev *et al*., 2013), the calculated activation energy of ozone decomposition reaction on the surface of manganese oxide catalyst supported on titanium was 11 kJ.mol^{-1}. This value, as the previous cited one, is similar to reported literature data for manganese based catalysts (Radhakrishnan *et al*., 2001). Catalytic cycle of ozone decomposition on MnO_x/TiO_2 catalyst is proposed in Figure 3. This mechanism is based on similar scheme of catalytic ozone decomposition described notably in a paper (Radhakrishnan *et al*., 2001) and in several articles (Reed *et al*., 2005; Xi *at al*., 2005). The transformation of the manganese site from species (I) to (III) is indicative of an oxidation reaction. The structure numbered (II) in Figure 3 is likely a transition state for this first step in the ozone decomposition process. The transformation of species (III) to species (VI) in the proposed catalytic cycle is represented by the redox reaction: $O_3+Mn^{4+}+O^{2-}\rightarrow O_2+O_2^{2-}+Mn^{4+}$. The transition states for this reaction are species (IV) and (V) presented in the catalytic cycle. Finally, the transformation of species (VI) to (I) in the catalytic cycle consist of desorption step and the redox reaction for this step is: $Mn^{4+}+O_2^{2-}\rightarrow O_2+Mn^{2+}$.

Chemical reactions proceeding over heterogeneous α-alumina supported silver catalyst via the dissociative adsorption of O_3 that produces surface chemisorbed atomic oxygen in concentrations sufficiently high to promote oxidation have been described in another article

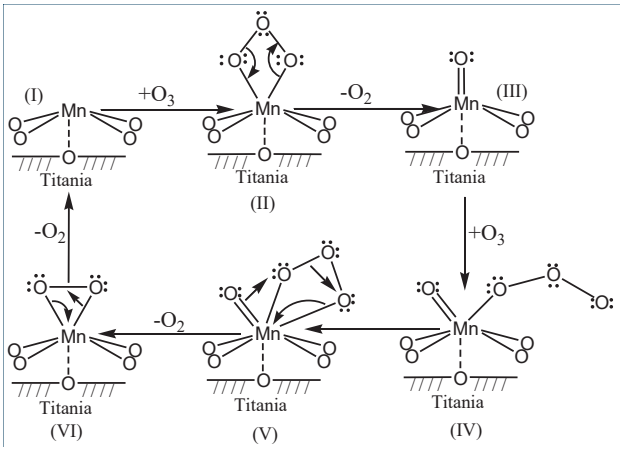

Figure 3. Catalytic cycle of ozone decomposition on MnO_x/TiO_2 catalyst.

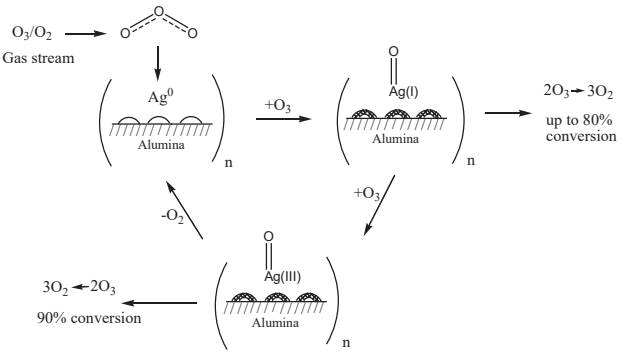

Figure 4. Mechanism of catalytic ozone decomposition on Ag/α-Al_2O_3 catalyst.

(Batakliev *et al.*, 2015). Catalytic scheme of ozone decomposition on Ag/Al_2O_3 catalyst was suggested in Figure 4. The transformation of the silver site from Ag^0 to Ag^{1+} oxidation state is indicative of the occurrence of an oxidation reaction. In this step the ozone conversion is up to 80%. During the next step the Ag^{1+} active site changes its valence state to Ag^{3+} and the ozone conversion becomes already 90%. In the final step of this catalytic cycle the silver active site is reduced and it returns back to the initial coordination state. The ability of silver to provide electrons during the reaction and its high concentration on the catalytic surface increase the probability of the supposed mechanism.

Ion-exchange preparation method of catalysts doped with transition metal was successfully applied for synthesis of materials tested in ozone decomposition reaction (Boevski *et al.*, 2011; Ma *et al.*, 2017). Considering the negative impact of water vapor over catalyst performance due to H_2O molecules adsorption (Batakliev *et al.*, 2008), the authors have studied the activity of cryptomelane-type manganese oxide octahedral molecular sieve (OMS-2) modified with cerium, cobalt and iron transition metal ions in destruction of ozone under high relative humidity. In fact, it has been reported that the structure, morphology, valence state of manganese species, and lattice parameters of OMS-2 can be tuned through single or/and multiple substitution of tunnel K^+ ions and framework Mn ions by different metal ions, such as Cu^{2+}, Ni^{2+}, Co^{2+}, Fe^{3+}, Cr^{3+} and Nb^{5+} (Pahalagedara *et al.*, 2014; Genuino *et al.*, 2015; Sun *et al.*, 2013). ICP-OES and XAFS results confirmed that Co^{3+} and Fe^{3+} replace Mn^{3+} in the cryptomelane structure and Ce^{4+} mainly exchanges the K^+ in the tunnel and partially replaces the Mn^{4+} in the framework of the cryptomelane structure. By using H_2-TPR experiments it was studied the reducibility of the catalysts. The final reduction of MnO_2 was found likely to be MnO with Mn_2O_3 and Mn_3O_4 as intermediates (Bai *et al.*, 2015). The mixed valence states as Mn^{4+} and Mn^{3+} in transition metal oxide samples are significant for electron transfer carrying out in the redox reactions of ozone decomposition catalytic cycle (Wang *et al.*, 2015). Mechanism of ozone decomposition process on the surface of transition metal doped OMS-2 has been presented on the following reaction scheme:

$$O_3 + [Mn^{3+}] \rightarrow O_2 + O^-_{ads}[Mn^{4+}] \quad (13)$$

$$O_3 + O^-_{ads}[Mn^{4+}] \rightarrow 2O_2 + [Mn^{3+}] \quad (14)$$

Plenty of Mn^{3+} active sites located on the catalytic surface could lead to formation of more surface oxygen vacancies, being a precondition for effective ozone decomposition (Jia *et al.*, 2016).

Sub-micrometer spherical $MnCO_3$ has been prepared via a facile co-precipitation method without additive agents at room temperature and characterized by several physical methods (Jia & Zhang, 2018). As-prepared $MnCO_3$ has showed better catalytic activity in ozone decomposition reaction than α-MnO_2 that is usually synthesized by a hydrothermal method (Dong *et al.*, 2014; Su *et al.*, 2013). By XPS analysis of the catalyst after ozonation, the authors have found amorphous MnO_x layer on the $MnCO_3$ surface playing role of active component in the catalytic ozone decomposition whereas the crystalline $MnCO_3$ serves to support stabilizing MnO_x surface phase. The chemical state of Mn was determined to rise from 2.15 to 2.32 during ozone treatment. *In-situ* Raman spectroscopy has been used to detect intermediates when $MnCO_3$ was exposed to the O_2 or O_3/O_2 flow. When the $MnCO_3$ was exposed to the O_3/O_2 flow, a distinct peak at 872 cm^{-1} appeared which could be ascribed to the O-O stretching mode of aggregated peroxide species (Jia *et al.*, 2016).

Catalytic activity of nanocomposites containing mono- and bimetallic Mn(II), Co(II), Cu(II), and Zn(II) complexes with Schiff bases [(salicyl-aldiminopropyl (L1) and 2-hydroxy-4-methoxybenzophenoniminopropyl (L2)] immobilized on silica in the reaction of ozone decomposition has been studied (Rakitskaya *et al.*, 2018). Using nanosilica as precursor for γ-aminopropylsilica synthesis, the authors have received immobilized Schiff bases (salicyl-aldiminopropyl and 2-hydroxy-4-methoxybenzophenoniminopropyl) through some well-known methods (Rakitskaya *et al.*, 2004) (Figure 5).

Monometallic $[M(L)_2]$ and bimetallic [Mn-M2-L] complexes have been obtained by adsorption of metal ions from ethanol, acetone or mixture of ethanol-acetone solutions. Best catalytic activity in ozone decomposition reaction has been found for the following complexes: $[Mn(L2)_2]$, [Mn-Cu-L2] and $[Mn(L1)_2]$.

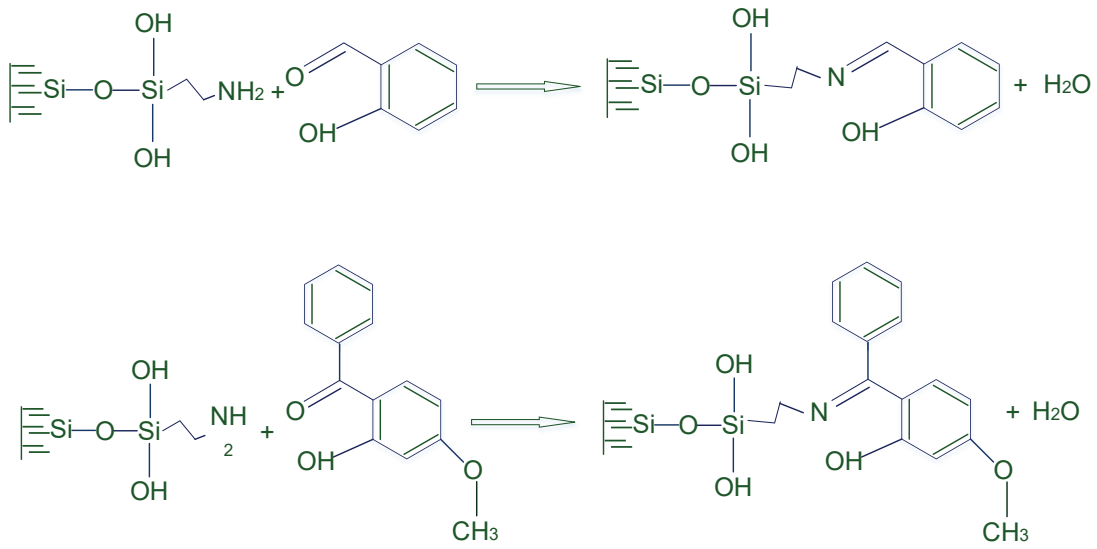

Figure 5. Scheme of immobilized Schiff bases fusion.

In another recent study, nitric acid-treated birnessite-type MnO_2 has been designed for humid ozone decomposition (Liu *et al.*, 2018). Detailed catalysts characterization showed that the higher amount of acid sites and oxygen vacancies together with their improved water-resistant properties facilitates adsorption and subsequent decomposition of humid O_3 over the H-MnO_2. The sample treated by nitric acid (H-MnO_2) exhibited stable O_3 conversion of ~50% within 24 h under 50% of relative humidity (115 ppm of O_3, 600 l g^{-1} h^{-1} of space velocity, 25 °C). The O_3 decomposition efficiency has been much higher over the H-MnO_2 than the pristine MnO_2 indicating that acid treatment could greatly enhance O_3 destruction. The authors ascribed the loss of K^+ cations to the exchange of H^+ into the catalyst layered structure during HNO_3 solution treatment. HNO_3 treatment greatly increased the S_{BET} to 228 m^2 g^{-1} that might be caused either by destabilization of the layered structure after proton exchange (Boppana *et al.*, 2013). XPS analysis has been made to define the oxidation state of surface manganese atoms as well as the nature of O 1s peaks. The Mn $2p_{3/2}$ peaks have given indication that Mn existed in a mixture of Mn^{3+} and Mn^{4+}. Based on the rule of electroneutrality, the higher Mn^{3+}/Mn^{4+} ratio would imply existence of more oxygen vacancies. Therefore, it has been suggested that the oxygen vacancies increased via acid treatment. Water adsorption experiments were performed on a thermogravimetric analyzer over pristine and acid-treated MnO_2. The normalized amount of water adsorption was calculated to be 1.48 mgH_2O/m^2 of catalyst and 0.32 mgH_2O/m^2 of catalyst for pristine and acid-treated MnO_2, respectively, indicating that the acid-treated MnO_2 was much more water-resistant than the pristine MnO_2.

A mechanism involving acid sites and oxygen vacancies for gaseous O_3 decmposition has been illustrated in Figure 6. Ozone molecule is first adsorbed on the surface acid site via latter oxygen atom through hydrogen bond. Then another uttermost oxygen atom of the O_3 molecule

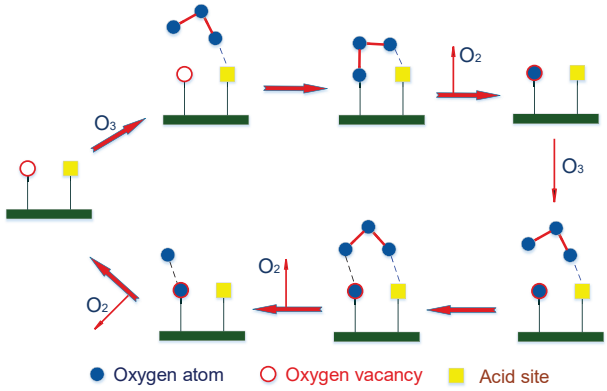

Figure 6. Alleged reaction pathway for gaseous O_3 decomposition.

fall down into an oxygen vacancy site, followed by formation of an O^{2-} species with release of an oxygen molecule into gas phase, and consequently, the acid site is regenerated. After that another one O_3 molecule creates hydrogen bond with surface acid site and the relevant oxygen atom interacts with the formed O^{2-} species to produce peroxide (O_2^{2-}) with simultaneous release of an oxygen molecule. Finally, the O_2^{2-} decomposes desorbing an oxygen molecule and the oxygen vacancy site is therefore regenerated.

The enhancement of the ratio Mn^{3+}/Mn^{4+} due to formation of oxygen vacancies has changed the charge distribution on α-MnO_2 nanofiber catalyst, resulting in an increment of ozone adsorption on the catalytic surface (Zhu *et al.* 2017). DFT calculation revealed that these vacancies could be accepted as active centers for ozone adsorption and afterwards decomposition. The authors have presented possible mechanism referring to such type active site for dry ozone decomposition, see Figure 7. The redox process consisted of three important steps: creation of active oxygen species O^{2-} by electron transfer effect,

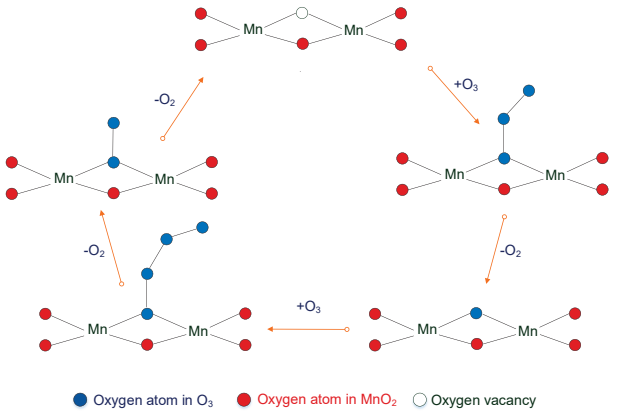

Figure 7. Mechanism of ozone decomposition on α-MnO_2 nanofiber catalyst under dry O_3/O_2 gas flow.

then second step oxidation by ozone generating peroxide species O_2^{2-}, followed finally by their reduction on manganese metal site and release of oxygen molecule.

Efficient catalytic composite system for ozone destruction has been reported notwithstanding the removed amount of ozone was barely 20 ppm O_3/air (Gong *et al.*, 2018). The ozone conversion at high relative humidity levels (ca. 90%) has been found to be above 96%. The excellent performance has been attributed to the highly active ultrafine Cu_2O nanoparticles heterogeneously nucleated on rGO. Cu_2O/rGO composite has exhibited the best catalytic activity in the decomposition of ozone, and this efficiency remained 100% after 10 h of continuous operation in dry air conditions. To explore ozone decomposition mechanism of the highly active Cu_2O/rGO catalyst, the surface states of used Cu_2O/rGO (still active) and that of used pure Cu_2O (deactivated) have been determined by XPS analysis. It was suggested that surface Cu(I) oxidation would not be the main reason for catalyst deactivation. Instead, the generated surface adsorbed oxygen species, during ozone decomposition, cover the active sites of the catalyst surface thus leading to the deactivation of the catalyst. It has been reported that graphene having defects and introduced into the catalyst could promote charge transport and favor activating of reactive molecular species (Gao *et al.*, 2013). The high catalytic activity of Cu_2O/rGO composite was attributed to some synergistic effect between the rGO and ultrafine Cu_2O solid phases that is likely to facilitate the needed electron density transfer in the catalytic process.

Ozone decomposition on copper oxide (CuO_x) with granular activated carbon (GAC) as a support catalyst has been studied in research article (Azhariyah *et al.*, 2018). CuO_x/GAC catalyst with size of 60–100 mesh and loading percentage of 2 wt% was found to have the highest conversion value being reached 100% but at relatively low ozone concentration of 36 ppm. The same Granular Activated Carbon as well as Natural Zeolite (NZ), and Green Sand (GS) have been used for catalytic supports in ozone decomposition reaction (Azhariyah *et al.*, 2018). Active sites comparison has been made using CuO_x and ZnO as metal oxides synthesized over the Granular Activated Carbon. CuO_x/GAC and ZnO/GAC with 2wt% active component in the catalyst structure have showed the highest catalytic activity decomposing 100% of 0.388 mg O_3/min.

If Cu-loaded materials for heterogeneous catalytic ozonation have been prepared by electroless plating-calcination, the deposition rate of metal could be controlled through adjusting the preparation conditions or additive agents in electroless plating process. Moreover, electroless plating might deposit Cu uniformly and densely on the surface of support materials that would result in better catalytic activity compared with those prepared by impregnation (Ren & Lai, 2016). Furthermore, it has been reported that adhesion between the Cu coating and support material obtained by electroless plating would also be much stronger than that of impregnation (Ren *et al.*, 2018). The authors suggested much better electroless plating-calcination comparing to the impregnation-calcination related with Cu-loaded material preparation for applying in catalytic ozonation process. The Cu/Al_2O_3 catalyst synthesized by electroless plating-calcination had uniform and dense deposition of the copper oxide phases on the support surface. Catalytic activity results confirmed the advantage of electroless plating-calcination preparation method showing higher performance of the new Cu/Al_2O_3 catalyst in COD removal during catalytic ozonation of 500 mg/l ρ-nitrophenol in aqueous solution.

According to defined by UV-Vis spectral analysis intermediates, it has been proposed ρ-nitrophenol degradation pathway as result of ozone treatment in presence of Cu/Al_2O_3 catalyst (Figure 8).

Transition metals-modified zeolite has been investigated as environmental catalyst for indoor air ozone decomposition (Mohamed *at al.*, 2018). In terms of O_3 removal efficiency, zeolite-based samples were ranked as follows: Fe-ZSM-5>Cu-ZSM-5>parent ZSM-5. The results revealed about 90% of 13 g/m^3 initial O_3 concentration removal efficiency for Fe-ZSM-5 and 70% for Cu-ZSM-5 as compared to nearly 40% for the parent zeolite. The samples activity has been explained by presence of free Fe and Cu catalytic sites where the exchanged metal ions are coordinated to six-member oxygen rings of aluminum tetrahedra. Removal of the extra-lattice oxygen atoms during high temperature catalyst pre-treatment could result in surface reduction. The following ozone oxidation of these transition metal active centers usually creates highly reactive oxygen species (Mortier, 1982). Some transition metal oxides are able to get involved at redox processes and could be used as reliable catalysts in ozone decomposition reaction. Mechanism based on redox couples including Cu^{+}-Cu^{2+} and Fe^{2+}-Fe^{3+} has been proposed:

$$O_3 + \{M^{n+} - Z\} \rightarrow O_2 + O^{-}\{M^{n+1} - Z\} \quad (15)$$

$$O_3 + O^{-}\{M^{n+1} - Z\} \rightarrow 2O_2 + \{M^{n+} - Z\} \quad (16)$$

where: M is Cu or Fe and Z is zeolite type ZSM-5.

The reported relatively good activity in ozone destruction of zeolite-based catalysts has been attributed to formation of framework Al-O-M (M: Cu or Fe) as well as to

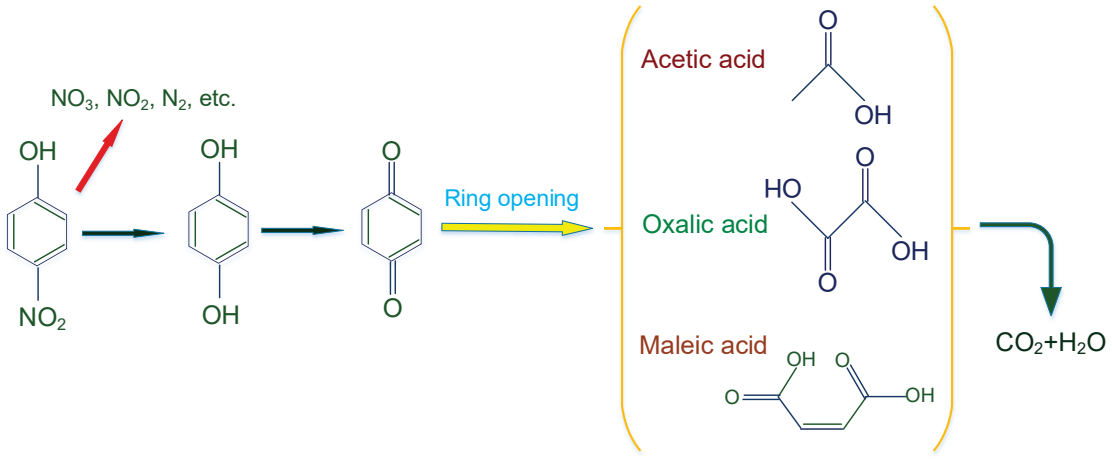

Figure 8. Proposed reaction pathway for the degradation of PNP by O_3 + Cu/Al_2O_3 prepared by electroless plating-calcination system.

alleged synergistic effect between zeolite and metal active sites improving ozone conversion on the catalytic surface.

Simultaneous catalytic decomposition of formaldehyde and ozone over manganese cerium oxides at room temperature has been examined depending on relative humidity of the gas stream passing by continuous-flow fixed-bed reactor under atmospheric pressure (Zhang *et al.*, 2018). The catalytic activity of $MnCeO_x$ catalyst has been compared with the solo MnO_x and CeO_2 catalysts to clarify the promotional effect of the formation of Mn-Ce solid solution on the catalytic activities. Investigation of the oxygen mobility and oxygen vacancies of the catalysts was carried out by O_2-TPD analysis. The spectral peaks have been attributed to physical adsorption of O_2 molecules, molecular oxygen species adsorbed on surface oxygen vacancy (O_I : O_2^-, O_2^{2-}), atomic oxygen species adsorbed on surface oxygen vacancy (O_{II} : O^-, O^{2-}, O^*), and lattice oxygen on the catalyst surface (O_{III}), respectively. In humid environment, the presence of water vapor creates surface hydroxyl groups resulting in the complete oxidation of most formaldehyde in the flow stream over $MnCeO_x$ catalyst at room temperature. That process is fed from the interaction between adsorbed water molecules with surface oxygen species generated from decomposition of ozone on the catalyst surface. *In situ* DRIFT spectrum of HCHO adsorption on $MnCeO_x$ catalyst has shown that after ozone inducement the absorbance at 3654 cm^{-1}, assigned to the OH stretching vibration ν(OH) of structural hydroxyl groups, significantly increases due to surface hydroxyl groups regeneration as result of HCHO and O_3 reaction on the catalyst surface. The absorbance of surface adsorbed water also continuously increased along with the reaction time growing and the absorbance at 3267 cm^{-1} was assigned to the OH stretching vibration ν(OH) of carboxylic acids.

NiO_x, CoO_x and MnO_x transition metal oxide catalysts have been allowed to the decomposition of toxic by-products as ozone (O_3) and nitrogen oxides (NO_x), formed in non-thermal plasma processes for indoor air treatment (Chen *et al.*, 2018). The 5 wt% MnO_x/Al_2O_3 catalyst was impregnated with different trichloro(alkyl)silanes in order to improve the ozone removal efficiency at 60% relative humidity in the air environment. As a ceramic material made from metal oxide, Al_2O_3 is hydrophilic in nature thank to the presence of hydroxyl groups on its surface (Kujawa *et al.*, 2015). The hydrophilic surface of alumina can be changed to a hydrophobic property by a surface modification treatment. Organosilanes such as methyl-, linear alkyl-, aromatic, and perfluorinated alkylsilanes are the most widely used materials for hydrophobic surface modification (Esmaeilirad *et al.*, 2016). Trichloro(alkyl) silanes possess three major parts: an organo-functional group, a linker and hydrolysable groups, which can be hydrolyzed and condensed to oligomers during the modification process. Stable covalent bonds could be created between the hydrolysable groups of the modifying agent and the hydroxyl groups on the substrate. The aliphatic hydrocarbon substituent changes the surface character of a ceramic material from hydrophilic to hydrophobic. A new mechanism based on some previous research (Tidahy *et al.*, 2007) for O_3 decomposition on the surface of γ-Al_2O_3 supported transition metal oxide catalyst was alleged:

$$O_3 + M^{n+} \rightarrow O^{2-} + M^{(n+2)+} + O_2 \quad (17)$$

$$O_3 + O^{2-} + M^{(n+2)+} \rightarrow O_2^{2-} + M^{(n+2)+} + O_2 \quad (18)$$

$$O_2^{2-} + M^{(n+2)+} \rightarrow O_2 + M^{n+} \quad (19)$$

The process of NO oxidation by ozone in presence of TiO_2 catalyst has been investigated at diverse NO inlet concentrations, gas flow rates and reactor temperatures (Jõgi *et al.*, 2016). Independent of reaction conditions and presence of catalyst, NO was totally oxidized to NO_2 when the inlet O_3 concentration reached the value of the inlet NO concentration. Further rise of inlet O_3 concentration resulted in oxidation of NO_2 to N_2O_5. The effect of TiO_2 catalyst appeared at higher reactor temperatures where the presence of TiO_2 increased the oxidation efficiency of NO_2 to N_2O_5 promoted by the presence of oxygen species created on the surface by catalytic decomposition of ozone. The oxidation of NO to NO_2 has been reported to be almost stoichiometric i.e. one O_3 molecule spun out

for one NO molecule (Mok, 2006). Further oxidation of NO_2 to N_2O_5 was less efficient and required either surplus amount of ozone or more continuous reaction time (Skalska *et al.*, 2012). The catalytic gas phase oxidation of NO_2 to N_2O_5 at 100 °C was limited by the formation of NO_3. The authors suggested that the additional formation of NO_3 takes place by the reaction between NO_2 and oxygen atoms stored on the TiO_2 surface: $NO_2+O \rightarrow NO_3$. These stored oxygen atoms are most likely formed as result of the ozone decomposition on TiO_2 surface: $O_3(g) \rightarrow O_2(g)+O$.

Catalytic ozone decomposition in gas-solids circulating fluidized-bed (CFB) riser has been investigated using computational fluid dynamics modeling (Kong *et al.*, 2013). The reaction was implemented on iron-impregnated fluid catalytic cracking particles and it was defined as a one-step first-order reaction: $O_3 \xrightarrow{\text{catalyst}} 1.5O_2$. During the fluidization process in a CFB, a catalytic ozone decomposition into diatomic oxygen required low concentrations of ozone so that the gas density and temperature changes caused by the reaction in the CFB could be overlooked. The simulation results have been compared with experimental data and the reaction rate was modified by using an empirical coefficient to provide better simulation results than the original reaction rate. It was found that particle size has great effect on the reaction rate redounded by the contact surface area in gas-solids interface.

Effective copper and manganese grafting over commercial titanium dioxide was reported to increase significantly the photocatalyst ozone decomposition rate (Patzsch&Bloh, 2018). Iron grafting appeared to be the most universal method of improving the photocatalytic ozone removal rate as even extremely low iron grafting ratios of 0.002 at.% were found to be sufficient to dramatically improve the catalyst performance. The means of ozone on NO_x-based air pollution is considerable because of the NO_2 formation by ozone initiated oxidation reactions. Direct NO_x abatement on titanium dioxide is quite challenging as the reaction involves several toxic intermediates, which may be released in the process (Bloh *et al.*, 2014). González-Elipe and co-workers shown that ozone can be photocatalytically decomposed on UV illuminated titanium dioxide surfaces (González-Elipe *et al.*, 1981). Mechanism of the redox process, including some short-lived intermediates and confirmed by EPR spectroscopy, is presented below:

$$OH^- + h^+ \rightarrow OH^\bullet + e^- \quad (20)$$
$$O_3 + e^- \rightarrow O_3^- \quad (21)$$
$$O_3 + OH^\bullet \rightarrow O_4^- + H^+ \quad (22)$$
$$O_3^- + O_3 \rightarrow O_2 + O_4^- \quad (23)$$
$$2O_3^- \rightarrow O_2 + 2O_2^- \quad (24)$$
$$O_4^- \rightarrow O_2 + O_2^- \quad (25)$$

This study has showed that ozone decomposition efficiency as simple and inexpensive method could improve the overall air cleaning properties of the photocatalyst. The authors explored the strategy of transition-metal grafting to increase the ozone-photo-degradation rate of titanium dioxide based photocatalysts. This grafting process has been reported to enhance the UVA as well as the visible light activity of many photocatalysts as the transition metal ions are strongly adsorbed onto the host crystals where they form small isolated ions or clusters facilitating this way charge carrier separation and electron transfer kinetics (Irie *et al.*, 2008; Liu *et al.*, 2012; Nishikawa *et al.*, 2013). It should be mentioned that the photocatalysts modified with Cu, Mn and Fe ions have been tested in ozone decomposition reaction applying relatively low inlet ozone concentration of 1 ppm.

Zinc oxide, as active phase, and granular activated carbon, as support, have been combined in catalyst for gas phase ozone destruction (Pradyasti *et al.*, 2018). The reaction was performed at room temperature and atmospheric pressure using fixed bed reactor. Crystal phase analysis of the catalysts before and after calcination at 300 °C has been studied by X-ray diffraction (XRD). The catalyst structure was found to be $ZnCO_3$ prior to thermal treatment and ZnO-after thermal treatment. Impurities located on the catalytic surface have been removed by HCl and NaOH processing, improving that way the activity of the ZnO/GAC catalyst in ozone decomposition reaction. Another application of activated carbon (AC) used as MnO_x catalyst support has been reported in a paper depicting the effects of Mn loading on the catalytic structure and ozone decomposition activity (Wang *et al.*, 2014). The catalytic activity was linked with the morphology and MnO_x content. The catalyst having 1.1wt% MnO_x exhibited better performance in ozone destruction because of its porous lichen-like structure compared to the compact morphology and ticker MnO_x layer of 11wt% MnOx/AC catalytic sample.

Catalytic ozone decomposition in water

In recent article (Li *et al.*, 2018), a Fe-based catalyst has been used as a heterogeneous catalyst for ozonation of industrial wastewater and some key operational parameters (pH and catalyst dosage) have been studied. It has been found indication of significantly improved mineralization of organic pollutants in wastewater. TOC removal was reported to be 78.7% at catalyst concentration of 200 g/l and 31.6% at ozonation without presence of catalyst. The Fe-based catalyst has promoted 70% ozone conversion into molecular oxygen in aqueous solution. Through characterization by SEM-EDS, XRD and XPS, it was suggested that FeOOH being on the catalyst surface was the main contributor to catalytic efficiency. Initial pH is one of the most important factors influencing the efficiency of ozonation in water. The authors claim that COD removal is much higher at pH 6 and 8 than that at pH 6.81 and 9, which indicated that COD treatment was much better in weak acid and weak base solutions. However, the Fe-based catalyst could be positively effective at pH 6–9 (Oputu *et al.*, 2015; Ghasemi *et al.*, 2016; Hadavifar *et al.*, 2016). Meanwhile, high pH means the presence of a significant concentration of hydroxyl anions (OH^-) that was confirmed to be an initiator for the decomposition of ozone reflecting in formation of OH radicals

(Staehelin&Hoigne, 1982). Hydroxyl radicals have been detected through EPR technology directly and $NaHCO_3$ scavenging experiments indirectly. It was verified that $HO^{\bullet}$ is a great contributor to mineralization of organic pollutants. The Fe-based catalyst was found to promote ozone decomposition in aqueous solution, which could be responsible for generation of $HO^{\bullet}$.

Synergistically, catalytic effect between $Mn^{4+/3+}$ and $Ce^{4+/3+}$ redox couples in manganese-cerium mixed oxides supported on practicable mesoporous γ-Al_2O_3 has been described in terms of catalyst surface properties and performance as well as reaction mechanism and kinetics during catalytic ozonation of bromaminic acid (BAA) in water solution (Wu *et al.*, 2018). The contribution of $Mn^{4+/3+}$ and $Ce^{4+/3+}$ redox couples to oxygen vacancies formation is presented on Figure 9(A). These oxygen vacancies could work as catalytic active sites for adsorption of ozone molecules that further would decompose via electron transfer from surface $Ce^{3+}$and Mn^{3+} species to create strong $HO^{\bullet}$ and $O_2^{\bullet-}$ radicals as depicted on Figure 9(B). Possible degradation pathway of 1-amino-4-bromoanthraquinone-2-sulfonic acid via Mn-CeO_x/γ-Al_2O_3-catalyzed ozonation was suggested in Figure 10.

BAA degradation mechanism through Mn-CeO_x/γ-Al_2O_3 catalyzed ozonation was based on important information about intermediates generation obtained by monitoring pH changes during single and catalytic ozonation as well as on intermediates identification by LC-MS analysis. The authors reported that during catalyzed ozonation the larger final pH of the solution is mainly due to generation of $HO^{\bullet}$ and $O_2^{\bullet}$ radicals, which could mineralize the acidic intermediates effectively. The adsorption of water molecules onto surface Lewis acid sites leads to their dissociation into protonated surface hydroxyl groups OH_2^+ bonded on catalyst surface, see Figure 9(B). Then the aqueous ozone molecules can interact with Brønsted acid $S–OH_2^+$ (S refers to catalyst surface) forming surface complex $S–OH_2^+–O_3$ via hydrogen bonding and/or electrostatic forces, due to the electrophilic and nucleophilic resonance structure of the ozone molecule (Qi *et al.*, 2010; Larachi *et al.*, 2002).

Summary and perspective

This review was focused on the mechanism of gas phase ozone decomposition process mostly considering optional reaction pathways based on short-lived molecular and atomic oxygen species acting as intermediates. The ozone decomposition in water environment could enhance the formation of hydroxyl radicals that play significant role in the process of water pollutants removal. Nowadays, highly efficient ozone decomposition is still representing a technological challenge especially in the presence of

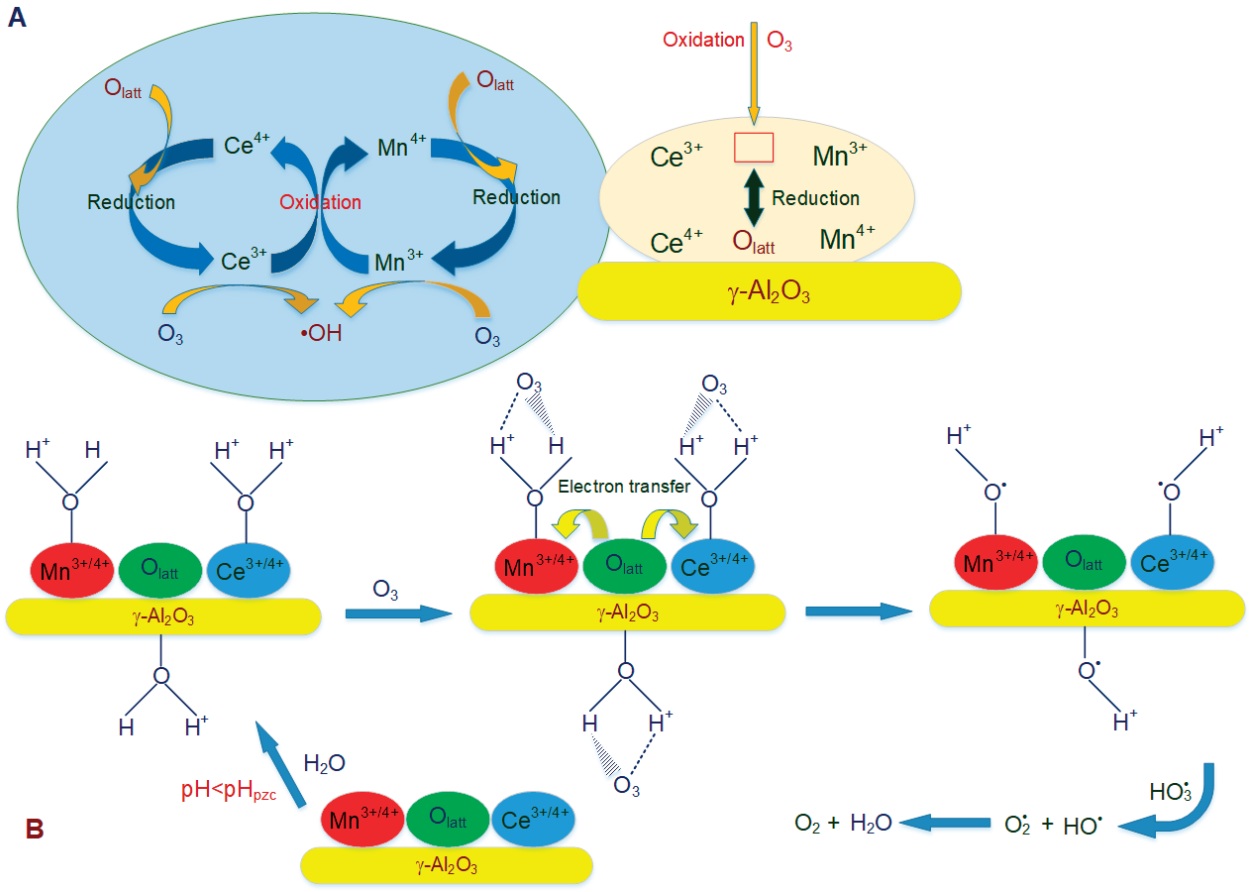

Figure 9. Scheme of Mn–CeO_x synergistic effect in catalytic process (a); and Alleged ozone decomposition mechanism on the surface of Mn–CeO_x/γ-Al_2O_3 catalyst (b).

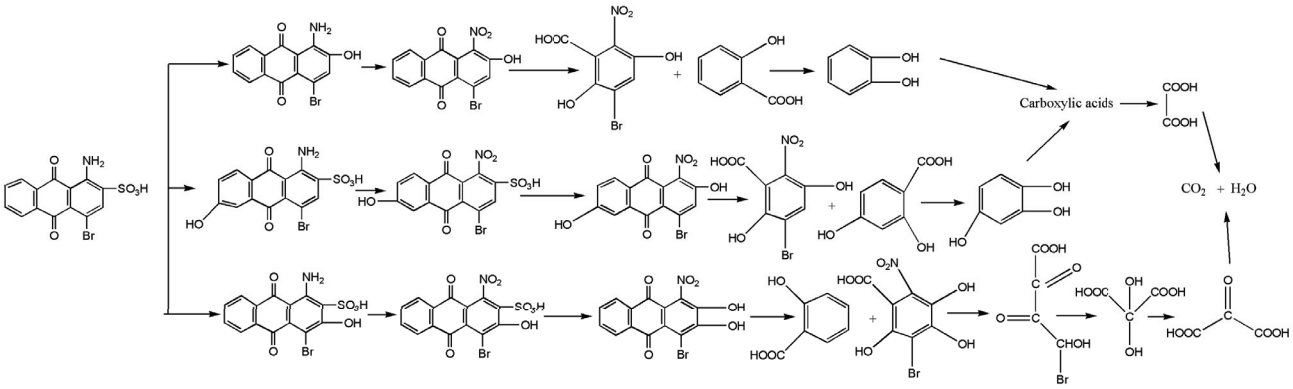

Figure 10. Suggested BAA degradation routes by the Mn-CeO_x/γ-Al_2O_3-catalyzed ozonation.

high humidity levels. The effect of water vapor is probably a result of thin film formation on the catalytic surface thus making the diffusion of ozone to the catalytic active centers more difficult. The synthesis of mixed oxide solid solution based on transition metals could create strong synergistic effect and give rise to larger number of adsorbed ozone molecules participating in preferable low temperature redox catalytic cycle that makes a great contribution to its superior activity. The physical characterization of metal oxide catalysts forming solid solution disclosed significant profusion of oxygen vacancies and surface lattice oxygen species improving the catalytic adsorption and redox properties. The main perspective in ozone decomposition research remains the *"in situ"* detection of all intermediate species generated and participating in the catalytic cycle of the reaction process using appropriate physical methods that should be applied with innovative and reliable experimental set-up. Deep kinetics investigations, including probable new models, have to be used in order to clarify the ozone degradation pathway on the surface of metal oxide catalysts.

REFERENCES

Azhariyah AS, Pradyasti A, Bismo S. (2018). Preparation and characterization of copper oxide catalyst with activated carbon support for ozone decomposition in industrial environment. *IOP Conf. Series: Earth and Environmental Science* **105**: 012012.

Azhariyah AS, Pradyasti A, Dianty AG, Bismo S. (2018). Comparative study of activated carbon, natural zeolite, and green sand supports for CuO_x and ZnO sites as ozone decomposition catalyst. *IOP Conf. Series: Earth and Environmental Science* **334**: 012075.

Bai B, Li J, Hao J. (2015). 1D–MnO_2, 2D–MnO_2 and 3D–MnO_2 for low–temperature oxidation of ethanol. *Appl Catal B Environ* **164**: 241–250.

Batakliev T, Rakovsky S, Zaikov G.E. (2008). Investigation of metal oxide catalyst in ozone decomposition. *Oxidation Communications* **31** (1): 145–150.

Batakliev T, Georgiev V, Anachkov M, Rakovsky S, Zaikov GE. (2014). Ozone decomposition. *Interdiscip Toxicol* **7**(2): 47–59.

Batakliev T, Georgiev V, Karakashkova P, Gabrovska M, Nikolova D, Anachkov M, Rakovsky S. (2017). Gas phase ozone decomposition over co-precipitated Ni-based catalysts. *Bulg Chem Commun* **49**(Special Issue L): 24–29.

Batakliev T, Tyuliev G, Georgiev V, Eliyas A, Anachkov M, Rakovsky S. (2015). Ozone decomposition reaction over α-alumina supported silver catalyst: comparative study of catalytic surface reactivity. *Ozone Sci Eng* **37**: 216–220.

Boevski I, Genov K, Boevska N, Milenova K, Batakliev T, Georgiev V, Nikolov P, Sarker DK. (2011). Low temperature ozone decomposition on Cu^{2+}, Zn^{2+} and Mn^{2+} – exchanged clinoptilolite. *CR ACAD BULG SCI* **64**(1): 33–38.

Bianchi CL, Pirola C, Ragaini V, Selli E. (2006). Mechanism and efficiency of atrazine degradation under combined oxidation processes. *Appl Catal B Environ* **64**: 131–138.

Bloh JZ, Folli A, Macphee DE. (2014). Photocatalytic NO_x abatement: why the selectivity matters. *RSC Adv* **4**: 45726–45734.

Boppana VBR, Yusuf S, Hutchings GS, Jiao F. (2013). Nanostructured alkaline–cation–containing δ–MnO_2 for photocatalytic water oxidation. *Adv Funct Mater* **23**: 878–884.

Chen C, Zhao B, Weschler CJ. (2012). Assessing the influence of indoor exposure to "outdoor ozone" on the relationship between ozone and short-term mortality in US communities. *Environ Health Perspect* **120**: 235–240.

Chen L, Ondarts M, Outin J, Gonthier Y, Gonze E. (2018). Catalytic decomposition performance for O_3 and NO_2 in humid indoor air on a MnO_x/Al_2O_3 catalyst modified by a cost-effective chemical grafting method. *J Environ Sci* **74**: 58–70.

Claudia C, Mincione E, Saladino R, Nicoletti R. (1994). Oxidation of Substituted 2-Thiouracils and Pyramidine-2-Thione with Ozone and 3,3-Dimethyl-1,2-Dioxiran. *Tetrahedron* **50**(10): 3259–3272.

Deninno MP, McCarthy KE. (1997). The C-14 radiolabelled synthesis of the cholesterol absorption inhibitor CP-148,623. A novel method for the incorporation of a C-14 label in enones. *Tetrahedron* **53**(32): 11007–11020.

Dong Y, Kun L, Jiang P, Wang G, Miao H, Zhang J, Zhang C. (2014). Simple Hydrothermal Preparation of Alpha–, Beta–, and Gamma–MnO_2 and Phase Sensitivity in Catalytic Ozonation. *RSC Adv.* **4**(74): 39167–39173.

Einaga H, Harada M, Futamura S. (2005). Structural Changes in Alumina-supported Manganese Oxides during Ozone Decomposition. *Chem. Phys. Lett.* **408**: 377.

Esmaeilirad A, Rukosuyev MV, Jun MBG, Van Veggel FCJM. (2016). A cost-effective method to create physically and thermally stable and storable superhydrophobic aluminum alloy surfaces. *Surf. Coat. Technol.* **285**: 227–234.

Gao E, Wang W. (2013). Role of graphene on the surface chemical reactions of $BiPO_4$–rGO with low OH–related defects, *Nano* **5**: 11248–11256.

Genuino HC, Seraji MS, Meng YT, Valencia D, Suib SL. Combined experimental and computational study of CO oxidation promoted by Nb in manganese oxide octahedral molecular sieves. (2015). *Appl Catal B Environ* **163**: 361–369.

Ghasemi Z, Younesi H, Zinatizadeh AA. (2016). Preparation, characterization and photocatalytic application of TiO_2/Fe-ZSM-5 nanocomposite for the treatment of petroleum refinery wastewater: optimization of process parameters by response surface methodology. *Chemosphere* **159**: 552–564.

Gong S, Chen J, Wu X, Nan N, Chen Y. (2018). *In-situ* synthesis of Cu_2O/reduced graphene oxide composite as effective catalyst for ozone decomposition. *Catal Commun* **106**: 25–29.

González-Elipe AR, Soria J, Munuera G. (1981). Photo-decomposition of ozone on TiO_2. *Zeitschrift Für Phys Chem* **126**: 251–257.

Hadavifar M, Younesi H, Zinatizadeh AA, Mahdad F, Li Q, Ghasemi Z. 2016. Application of integrated ozone and granular activated carbon for decolorization and chemical oxygen demand reduction of vinasse from alcohol distilleries. *J Environ Manag* **170**: 28–36.

Hata K, Horiuchi M, Takasaki T. (1988). Preparation of high performance metal catalyst. Jap Pat CA, 108, 61754u.

Irie H, Miura S, Kamiya K, Hashimoto K. (2008). Efficient visible light-sensitive photocatalysts: grafting Cu(II) ions onto TiO_2 and WO_3 photocatalysts. *Chem Phys Lett* **457**: 202–205.

Jia JB, Zhang PY, Chen L. (2016). Catalytic decomposition of gaseous ozone over manganese dioxides with different crystal structures. *Appl Catal B Environ* **189**: 210–218.

Jia J, Zhang P, Chen L. (2016). The Effect of Morphology of A–MnO_2 on Catalytic Decomposition of Gaseous Ozone. *Catal Sci Technol* **6**(15): 5841–7.

Jia J, Zhang P. (2018). Catalytic Decomposition of Airborne Ozone by $MnCO_3$ and its Mechanism, *Ozone Sci Eng* **40**(1): 21–28.

Jõgi I, Erme K, Raud J, Laan M. (2016). Oxidation of NO by ozone in the presence of TiO_2 catalyst, *Fuel* **173**: 45–51.

Kobayashi M, Mitsui M, Kiichiro K. (1988). Chemical composition of metal oxide catalysts. Jap Pat CA, 109, 175615a.

Kong L, Zhu J, Zhang C. (2014). Catalytic Ozone Decomposition in a Gas-Solids Circulating Fluidized-Bed Riser. *Chem Eng Technol* **37 (3)**: 435–444.

Kujawa J, Cerneaux S, Kujawski W. (2015). Highly hydrophobic ceramic membranes applied to the removal of volatile organic compounds in pervaporation. *Chem Eng J* **260**: 43–54.

Lai D, Karava P, Chen Q. (2015). Study of outdoor ozone penetration into buildings through ventilation and infiltration. *Build Environ* **93**: 112–118.

Larachi F, Pierre J, Adnot A, Bernis A. (2002). Ce 3d XPS study of composite $Ce_xMn_{1-x}O_{2-y}$ wet oxidation catalysts. *Appl Surf Sci* **195**: 236–250.

Li X, Chen W, Ma L, Wang H, Fan J. (2018). Industrial wastewater advanced treatment via catalytic ozonation with a Fe-based catalyst, *Chemosphere* **195**: 336–343.

Liu G, Yin L-C, Wang J, Niu P, Zhen C, Xie Y, Cheng H–M. (2012). A red anatase TiO_2 photocatalyst for solar energy conversion. *Energy Environ Sci* **5**: 9603.

Liu Y, Yang W, Zhang P, Zhang J. (2018). Nitric acid-treated birnessite-type MnO_2: An efficient and hydrophobic material for humid ozone decomposition. *Appl Surf Sci* **442**: 640–649.

Lunin VV, Popovich MP, Tkachenko SN. (1998). Physical Chemistry of Ozone. Moscow State University Publisher, 480 p. [in Russian].

Ma J, Sui MH, Chen ZL, Li NW. (2004). Degradation of Refractory Organic Pollutants by Catalytic Ozonation—Activated Carbon and Mn-Loaded Activated Carbon as Catalysts. *Ozone Sci Eng* **26**(1): 3–10.

Ma J, Wang C, Hong H. (2017). Transition metal doped cryptomelane–type manganese oxide catalysts for ozone decomposition. *Appl Catal B Environ* **201**: 503–510.

Mohamed EF, Awad G, Zaitan H, Andriantsiferana C, Manero M–H. (2018). Transition metals-incorporated zeolites as environmental catalysts for indoor air ozone decomposition. *Environ Technol* **39**(7): 878–886.

Mok YS, Yoon EY. (2006). Effect of Ozone Injection on the Catalytic Reduction of Nitrogen Oxides. *Ozone Sci Eng* **28**: 105–110.

Mortier J. (1982). *Compilation of extra framework sites in zeolites*, Guildford: Butterworth Sci. Ltd., 67 p.

Nishikawa M, Hiura S, Mitani Y, Nosaka Y. (2013). Enhanced photocatalytic activity of $BiVO_4$ by co-grafting of metal ions and combining with $CuBi_2O_4$. *J Photochem Photobiol A Chem* **262**: 52–56.

Oohachi K, Fukutake T, Sunao T. (1993). Method for synthesis of iron oxides. Jap Pat CA, 119, 119194g.

Oputu O, Chowdhury M, Nyamayaro K, Fatoki O, Fester V. (2015). Catalytic activities of ultra-small beta-FeOOH nanorods in ozonation of 4-chlorophenol. *J Environ Sci* **35**: 83–90.

Oyama ST. (2000). Chemical and Catalytic Properties of Ozone. *Catal Rev Sci Eng* **42**: 279.

Pahalagedara LR, Dharmarathna S, King'ondu CK, Pahalagedara MN, Meng YT, Kuo CH, Suib SL. (2014). Microwave-Assisted Hydrothermal Synthesis of α-MnO_2: Lattice Expansion via Rapid Temperature Ramping and Framework Substitution. *J Phys Chem C* **118**: 20363–20373.

Patzsch J, Bloh J. (2018). Improved photocatalytic ozone abatement over transition metal-grafted titanium dioxide. *Catal Today* **300**: 2–11.

Perry RH, Green D. (1989). *Perry's Chemical Engineer's Handbook*, McGraw-Hill, New York, 147 p.

Pradyasti A, Azhariyah AS, Karamah EF, Bismo S. (2018). Preparation of zinc oxide catalyst with activated carbon support for ozone decomposition. *IOP Conf Ser Earth Environ Sci* **105**: 012013.

Qi F, Chu W, Xu B. (2016). Comparison of phenacetin degradation in aqueous solutions by catalytic ozonation with $CuFe_2O_4$ and its precursor: Surface properties, intermediates and reaction mechanisms. *Chem Eng J* **284**: 28–36.

Radhakrishnan R, Oyama ST, Chen J, Asakura A. (2001). Electron Transfer Effects in Ozone Decomposition on Supported Manganese Oxide. *J Phys Chem B* **105**(19): 4245–4253.

Rakitskaya T, Truba A, Radchenko E, Golub A. (2018). Mono- and Bimetallic Complexes of Mn(II), Co(II), Cu(II), AND Zn(II) with Schiff Bases Immobilized on Nanosilica as Catalysts in Ozone Decomposition Reaction, *Chem Chem Technol* **12**(1): 1–6.

Rakyts'ka T., Pidmazko A., Golub O. (2004). Compositions Based on Pl(II) and Cu(II) Compounds, Halide Ions, and Bentonite for Ozone Decomposition. *Ukr Khim Zh* **70**: 16 [in Ukrainians].

Rakovsky SK, Zaikov GE. (2007). *Kinetic and mechanism of ozone reactions with organic and polymeric compounds in liquid phase – 2nd edition*, Nova Sci. Publ., Inc. New York.

Reed C, Xi Y, Oyama ST. (2005). Distinguishing between reaction intermediates and spectators: a kinetic study of acetone oxidation using ozone on a silica-supported manganese oxide catalyst. *J Catal* **235**: 378–392.

Ren Y, Lai B. (2016). Comparative study on the characteristics, operational life and reactivity of Fe/Cu bimetallic particles prepared by electroless and displacement plating process. *RSC Adv* **6**: 58302–58314.

Ren Y, Li J, Peng J, Ji F, Lai B. (2018). Strengthening the catalytic activity for ozonation of Cu/Al_2O_3 by an electroless plating–calcination process. *Ind Eng Chem Res* **57**: 1815–1825.

Qi F, Xu B, Chen Z, Zhang L, Zhang P, Sun D. (2010). Mechanism investigation of catalyzed ozonation of 2-methylisoborneol in drinking water over aluminum (hydroxyl) oxides: Role of surface hydroxyl group. *Chem Eng J* **165**: 490–499.

Skalska K, Miller JS, Wilk M, Ledakowicz S. (2012). Nitrogen Oxides Ozonation as a Method for NO_x Emission Abatement. *Ozone Sci Eng* **34**: 252–258.

Skoumal M, Cabot PL, Centellas F, Arias C, Rodriguez RM, Garrido JA, Brillas E. (2006). *Appl Catal B Environ* **66**: 228–240.

Staehelin J, Hoigne J. (1982). Decomposition of ozone in water–rate of initiation by hydroxide ions and hydrogen–peroxide. *Environ Sci Technol* **16**: 676–681.

Su D, Ahn H–J, Wang G. (2013). Hydrothermal synthesis of α-MnO_2 and β-MnO_2 nanorods as high capacity cathode materials for sodium ion batteries. *J Mater Chem A* **1**: 4845–4850.

Sun M, Yu L, Ye F, Diao GQ, Yu Q, Hao ZF, Zheng YY, Yuan LX. (2013). Transition metal doped cryptomelane-type manganese oxide for low-temperature catalytic combustion of dimethyl ether. *Chem. Eng. J.* **220**: 320–327.

Tchihara S. (1988). Cobalt catalyst for decomposition of ozone. Jap Pat CA, 108, 192035h.

Terui S, Sadao K, Sano N, Nichikawa T. (1990). Synthesis of supported silver oxide catalysts. Jap Pat CA, 112, 20404p.

Terui S, Sadao K, Sano N, Nichikawa T. (1991). Investigation on Pd and Rh catalysts supported on colloidal polyurethane for ozone destruction. Jap Pat CA, 114, 108179b.

Tidahy HL, Siffert S, Wyrwalski F, Lamonier J–F, Aboukaïs A. (2007). Catalytic activity of copper and palladium based catalysts for toluene total oxidation. *Catal Today* **119**: 317–320.

Wang C, Ma J, Liu F, He H, Zhang R. (2015). The Effects of Mn^{2+} Precursors on the Structure and Ozone Decomposition Activity of Cryptomelane-Type Manganese Oxide (OMS–2) Catalysts. *J Phys Chem C* **119**: 23119–23126.

Wang M, Zhang P, Li J, Jiang C. (2014). The effects of Mn loading on the structure and ozone decomposition activity of MnOx supported on activated carbon. *Chinese J Catal* **35**: 335–341.

Wiley-VCH. (1991). *Ullmann's Encyclopedia of Industrial Chemistry*. John Wiley and Sons, New York.

Wu Z, Zhang G, Zhang R, Yang F. (2018). Insights into Mechanism of Catalytic Ozonation over Practicable Mesoporous Mn-CeO_x/γ-Al_2O_3 Catalysts. *Ind Eng Chem Res* **57**: 1943–1953.

Xi Y, Reed C, Lee Y–K, Oyama ST. (2005). Acetone oxidation using ozone on manganese oxide catalysts. *J Phys Chem B* **109**: 17587–17596.

Zavadskii AV, Kireev SG, Muhin VM, Tkachenko SN, Chebkin VV, Klushin VN, Teplyakov DE. (2002). Thermal Treatment Influence over Hopcalite Activity in Ozone Decomposition. *J Phys Chem* **76**: 2278 [in Russian].

Zhang Y, Chen M, Zhang Z, Jiang Z, Shangguan W, Einaga H. (2019). Simultaneously catalytic decomposition of formaldehyde and ozone over manganese cerium oxides at room temperature: Promotional effect of relative humidity on the $MnCeO_x$ solid solution. *Catal Today* **327**: 323–333.

Zhao L, Ma J, Sun ZZ. (2008). Oxidation products and pathway of ceramic honeycomb-catalyzed ozonation for the degradation of nitrobenzene in aqueous solution. *Appl Catal B Environ* **79**: 244–253.

ISSN: 1337-6853 *(print version)* | 1337-9569 *(electronic version)*